Catalysis Today 138 (2008) 110–116

Contents lists available at ScienceDirect

Catalysis Today

journal homepage: www.elsevier.com/locate/cattod

Photocatalytic degradation of chlorinated pyridines in titania aqueous suspensions

M.A. Aramendía, J.C. Colmenares, S. López-Fernández, A. Marinas *, J.M. Marinas, J.M. Moreno, F.J. Urbano

Departamento de Química Orgánica, Universidad de Córdoba, Edf. Marie Curie, Campus Universitario de Rabanales, E-14014 Córdoba, Spain

ARTICLE INFO

Article history:
Available online 9 June 2008

Keywords:
2-Chloropyridine
3-Chloropyridine
2,3-Dichloropyridine
Photocatalysis
Photocatalytic degradation
Mineralization

ABSTRACT

The photocatalytic degradation of 3-chloropyridine was studied using different titania-based catalysts, its disappearance followed a zero-order kinetics. In our conditions, complete mineralization of 100 ppm of 3-chloropyridine occurred within ca. 480 min of UV-radiation on bare-titania systems. Doping of titania with metals was detrimental for photocatalysis. Some reaction intermediates were identified by SPME–GC–MS and a tentative degradation pathway was proposed implying two parallel routes with hydroxylation and ring opening prior to or after the release of chloride ions. Unlike 3-chloropyridine, 2-chloropyridine degradation follows a first-order kinetics. Competitive reactions on solutions containing 3-chloropyridine and 2-chloropyridine evidenced the stronger adsorption of the latter compound. Finally, in a similar way as described for 3-chloropyridine, photocatalytic degradation of 2,3-dichloropyridine followed a zero-order kinetics. Moreover, detection of coupling products containing 3 chlorine atoms evidenced the existence of a radical mechanism.

1. Introduction

Emissions of halogenated organic compounds are associated with a wide range of industrial processes. Most of these compounds are toxic and present high carcinogenic and mutagenic activity. Therefore, development of efficient methods to dispose of them is important. Direct combustion requires temperatures within the range of 1073–1273 K. Thus, it is an expensive procedure which can lead, due to the presence of chlorine, to products from incomplete combustion which are extremely toxic. Catalytic oxidation at lower temperatures is a more suitable method [1]. Other procedures used are hydrodehalogenation by molecular hydrogen or hydrogen transfer [2], biodegradation [3] or photocatalysis [4,5]. The present piece of research is aimed at exploring photocatalytic degradation of several chloropyridines present in waters. These chemicals are important reaction intermediates in organic synthesis in pharmaceutical industry (antihystaminic or antirythmic compounds), or agrochemistry (fungicides and pyridine herbicides). At the beginning of the study 3-chloropyridine was taken as model of pyridine herbicides (picloram, aminopyralid or clopyralid) and the study was later extended to 2-chloropyridine and 2,3-dichloropyridine.

This work must be seen in the context of a project on the destruction of herbicides residues in water, a topic of paramount importance in Andalucia, a Spanish community highly dependent on agriculture.

2. Experimental

2.1. Chemicals

3-Chloropyridine (3-Clpy), 2-chloropyridine (2-Clpy) and 2,3-dichloropyridine (2,3-diClpy) (99% purity each) were provided by Sigma–Aldrich. 96% sulfuric acid, sodium nitrate, sodium nitrite, sodium chloride, ammonium fluoride, anhydrous sodium acetate, sodium hydroxide, 37% hydrochloric acid and L-(+)-tartaric acid were purchased from Panreac. Sodium carbonate and bicarbonate, 2,6-pyridinedicarboxilic acid (dipicolinic acid), sodium and ammonium formate were provided by Sigma–Aldrich. Finally, formic acid was provided by Merck.

All photocatalytic degradation assays were carried out using titania-based photocatalysts. Therefore, different titania-based systems doped with diverse transition metals (Ag, Fe, Pd, Pt, Zn and Zr) in a metal/Ti nominal ratio equal to 0.01, whose syntheses were described in a previous paper [6] were used. Such systems were synthesized through the sol–gel process (pH 9 with NH_4OH) using titanium tetraisopropoxide (TTIP) and the corresponding metal acetylacetonates as the titanium and metal precursors,

* Corresponding author. Tel.: +34 957218622; fax: +34 957212066.
E-mail address: alberto.marinas@uco.es (A. Marinas).

0920-5861/$ – see front matter © 2008 Elsevier B.V. All rights reserved.
doi:10.1016/j.cattod.2008.04.035

Table 1
Main features concerning characterization of the different titania-based solids used in the present work

Catalyst[a]	ICP-MS	N_2-isotherms	XRD	
	Experimental (metal/Ti %)	S_{BET} (m^2/g)	Crystal phases[b] (%)	Crystallite size of Anatase[c] (nm)
TiO_2-ST	–	35	A/R (97:3)	28
TiO_2-US	–	121	A (100)	19
TiO_2-(Ag)-ST	1.3	53	A (100)	21
TiO_2-(Ag)-US	1.7	58	A (100)	22
TiO_2-(Fe)-ST	1.8	48	A (100)	26
TiO_2-(Fe)-US	1.7	61	A (100)	20
TiO_2-(Pd)-ST	0.6	65	A (100)	23
TiO_2-(Pd)-US	0.6	75	A (100)	20
TiO_2-(Pt)-ST	0.3	40	A (100)	31
TiO_2-(Pt)-US	0.5	57	A (100)	23
TiO_2-(Zn)-ST	0.7	18	A/R (90:10)	31
TiO_2-(Zn)-US	0.7	59	A (100)	19
TiO_2-(Zr)-ST	0.8	65	A (100)	19
TiO_2-(Zr)-US	0.8	64	A (100)	21
Degussa P25[d]	–	51	A/R (83:17)	21

[a] Suffix ST or US refers to aging method (magnetic stirring or ultrasonic irradiation, respectively). The initials in brackets indicate the dopant. For further details see Ref. [6].
[b] Anatase (A) and rutile (R).
[c] Determined from (1 0 1) reflection using Scherrer equation.
[d] Data taken from Ref. [7].

respectively. The gels were aged under ultrasonic irradiation (US series) or magnetic stirring (ST series) for 24 h and calcined at 500 °C for 6 h in the air. Moreover, Degussa P25 was utilized for comparative purposes. The main features concerning characterization of all the systems are summarized in Table 1.

Water used for preparation of samples was Milli-Q quality water (Millipore Iberica, Spain).

2.2. Standard solutions

2-Clpy, 3-Clpy and 2,3-diClpy calibrations were carried out from water solutions in the range of 0–150 mg L^{-1} (r^2 = 0.9996), analyzed by HPLC–DAD.

Concerning anion detection, standard solutions containing $NaNO_3$ (nitrate determination), $NaNO_2$ (nitrite), NaCl (chloride), CH_3COONH_4 (acetate) and HCOONa (formic acid) in the range of 0–30 mg L^{-1} were prepared. Regarding ammonium detection, $HCOONH_4$ solutions (0–20 mg L^{-1}) were utilized. In all cases correlation coefficients obtained for calibration curves were over 0.99.

2.3. Photocatalysis experiments

All catalytic runs were performed in a Pyrex cylindrical doubled-walled immersion well reactor (23 cm long × 5 cm internal diameter, with a total volume of ca. 450 cm^3). Irradiation of the reaction solutions was carried out by using a medium pressure 125 W Hg lamp (λ_{max} = 365 nm) supplied by Photochemical Reactors Ltd. (Model 3010). Lamp output was calculated to be ca. 1.5×10^{-3} Einstein/s (potassium ferrioxalate actinometry). Water used for cooling was thermostated at 20 °C.

Constant agitation of the suspension was insured by a magnetic stirrer placed at the reactor base.

Solutions of pure chloropyridines were prepared in Milli-Q water and kept in the dark at 4 °C. Experiments were carried out from 200 mL of the mother solution (25–120 ppm) and 300 mg of TiO_2. The mixture was maintained in the dark for 20 min under stirring (500 rpm) to reach adsorption equilibrium, and was then irradiated. All degradation experiments were carried out at room temperature and unless otherwise stated bubbling through the suspension an O_2/N_2 (10:90, v/v) mixture at 80 mL min^{-1}.

2.4. Analyses

2.4.1. Kinetic studies

Samples taken at different times of irradiation were filtered through 0.22 μm, 25 mm ϕ nylon filters provided by Tracers, in order to remove TiO_2 particles before analyses by HPLC–DAD. A Waters 2695 liquid chromatograph equipped with a quaternary solvent delivery system, an autosampler and a Waters 2996 DAD detector (λ = 210 and 266 for 3-chloropyridine, 208 and 263 nm for 2-chloropyridine, 216 and 271 nm for 2,3-dichloropyridine) was used. For experiment starting from solutions containing only one of the analytes, separation was performed on a Tracer Kromasil100 C18 column (150 mm × 2.1 mm ID, 5 μm particle diameter) in the isocratic regime (CH_3CN/H_2O, 40:60, v/v, 0.3 mL min^{-1}). In the case of simultaneous determination of 2- and 3-chloropyridine, a gradient program was developed. The mobile phases were as follows: mobile phase A: acetonitrile; mobile phase B: 95:5 water/acetonitrile (v/v). The samples were eluted according to the following gradient: 0–6 min, 100% A; 6–11 min, 100–75% A; 11–13 min, 75% A; 13–15 min, 75–50% A; 15–22 min, 50% A; 22–26 min, 50–100% A; and 26–32 min, 100% A. The flow rate was set at 0.3 mL/min during the chromatographic process, the temperature of the analytical column was 30 °C and the injection volume 20 μL.

2.4.2. Mineralization studies

Evolution of inorganic ions (NO_3^-, NO_2^-, Cl^- and NH_4^+) together with $HCOO^-$ and CH_3COO- was followed by conductivity HPLC. Quantification was possible using the corresponding calibration curves. The HPLC system used comprised a Metrohm Metrosep anion dual 2 column (75 mm × 4.6 mm ID, 5 μm particle diameter), a Metrohm 753 ionic suppression module (using H_2SO_4 for regeneration of cartridges) and a Metrohm 732 ionic conductivity detector. Mobile phase was a mixture of Na_2CO_3 (1.3 mmol L^{-1}) and $NaHCO_3$ (2.0 mmol L^{-1}), flow rate 0.8 mL min^{-1}. Injection volume was 20 μL.

For ammonium ion determination, ion suppression module was not necessary and a Metrohm Metrosep C2 100 column (100 mm × 4.0 mm ID, 5 μm particle diameter) was used. Mobile phase was a mixture of dipicolinic acid (0.75 mmol L^{-1}) and L-(+)-tartaric acid (4 mmol L^{-1}), flow rate 1 mL min^{-1}. Injection volume was 10 μL.

CO_2 evolution was monitored by two different methods (i) on-line coupling of the reactor to a HP6890 gas chromatograph equipped with a six-way valve, a HP-PLOTU column (30 m long, 0.53 mm ID, 20 μm film thickness) and a Ni methanator (Agilent Part Number G2747A) thus determining CO_2 as methane; (ii) through the analysis of samples in a TOC apparatus (Rosemount analytical Dohrmann DC-190).

2.4.3. By-product evaluation

Reaction products were followed by SPME–GC–MS using a CP-3800 Gas Chromatograph connected to a Varian 1200 Quadrupole MS and provided with a CombiPal autosampler. A Supelcowax-10 capillary column (0.25 μm film, 60 m × 0.25 mm) was utilized. Injection temperature was 275 °C and the carrier gas (He) flow through the column was fixed at 1 mL/min. Oven temperature was kept at 90 °C for 3 min, raised up to 270 °C at 20 °C/min, the final temperature maintained for 20 min.

Different fibers were tested as adsorbents (polyacrylate, PDMS/DVB...). The best one had polyacrylate as the stationary phase

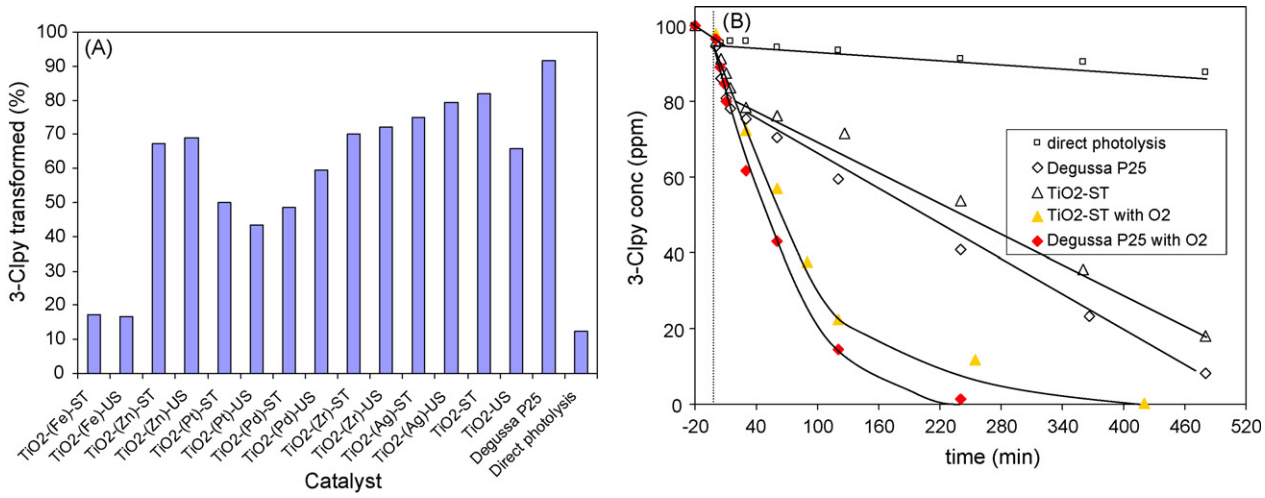

Fig. 1. Results obtained for photocatalytic degradation of 200 mL of an aqueous solution containing 100 ppm of 3-chloropyridine on 300 mg of catalyst. (A) Percentage of disappearance achieved with different titania-based systems after 8 h of UV irradiation in a reactor open to the air. (B) Comparative studies using TiO_2-ST and Degussa P25 with and without O_2 bubbling as well as for direct photolysis.

(Supelco 57305). Prior to use, the fiber was conditioned at 300 °C for 2 h. It was then introduced in the vial containing the filtered sample which was extracted at 40 °C and 500 rpm for 30 min. Masses were scanned in the 30–300 amu range. Moreover, selective extraction of ions helped us to detect the presence of low contents of certain intermediates in the total ion chromatogram. Main selected peaks were *m*/*z* 79 (pyridine), 113 and 115 (2- and 3-chloropyridine), 163 (2,3-dichloropyridine), 95 and 111 (hydroxylated pyridines), 129, 131, 145, 147, 161 and 163 (hydroxylated chloropyridines). Nevertheless, all the products were characterized by comparing the molecular ion and fragmentation pattern with those reported in the GC-MS library.

3. Results and discussion

3.1. Kinetics of 3-chloropyridine disappearance

The use of a diode array detector allowed us to check peak purity through simultaneous quantification at several wavelengths. In the case of 3-chloropyridine, determination was performed at 210 and 266 nm which corresponds to two absorption maxima in UV absorption spectrum of 3-chloropyridine. Fig. 1A shows the results found after 8 h UV irradiation for photocatalytic degradation of 3-chloropyridine (100 ppm aqueous solution) in a reactor open to the air, without O_2 bubbling. From that figure it is clear that the best results in terms of 3-Clpy disappearance are obtained with Degussa P25 and TiO_2-ST. Doping with Fe, Pd, Pt, Zr or Zn do not lead to any improvement in photoactivity. Instead, such doping is particularly detrimental in the case of iron. Moreover, a higher surface area does not ensure a higher activity, as evidenced by the fact that 3-Clpy degradation is faster with TiO_2-ST (35 m^2/g) than with TiO_2-US (135 m^2/g). Results found for this screening prompted us to select the most active systems Degussa P25 and TiO_2-ST for further studies on 3-Clpy photocatalytic degradation.

Fig. 1B shows a typical degradation kinetic curve for 3-chloropyridine (100 ppm aqueous solution) on both TiO_2-ST and Degussa P25 at 210 nm. Experiments were performed three times and the points correspond to the average of the repetitions. Empty symbols correspond to reactions carried out with the reactor open to the air whereas results obtained for experiments in which an O_2/N_2 (10:90) flow was bubbled through the suspension are represented with full symbols. The curves obtained at 266 nm were exactly the same, thus overlapping with those at 210 nm. As can be seen, there is hardly a reaction in the absence of catalyst (direct photolysis) thus concluding that the process is mainly photocatalytic. Moreover, reaction is significantly faster when O_2 is bubbled into the suspension. Finally, 3-Clpy disappearance is faster with Degussa P25 than with TiO_2-ST which prompted us to select the latter system, with O_2 bubbling, for more accurate kinetic studies.

Results obtained from experiments performed at different 3-Clpy initial concentrations in order to determine the substrate partial order are shown in Fig. 2. As can be seen, disappearance follows a zero kinetic order with a rate being constant, whatever the initial concentration, and equal to 1.9×10^{-5} mol L^{-1} min^{-1}.

Such a kinetics is consistent with resulted reported elsewhere for 3-amino-2-chloropyridine [8].

3.2. Mineralization evaluation

A complete degradation of an organic molecule by photocatalysis, normally leads to gaseous CO_2, and the heteroatoms turn into inorganic anions that remain in solution. From 3-chloropyridine

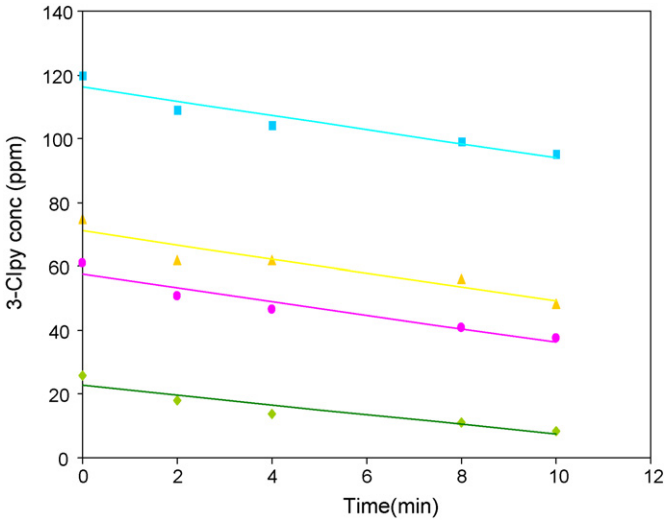

Fig. 2. Kinetic studies on TiO_2-ST evidencing the zero-order with respect to 3-chloropyridine.

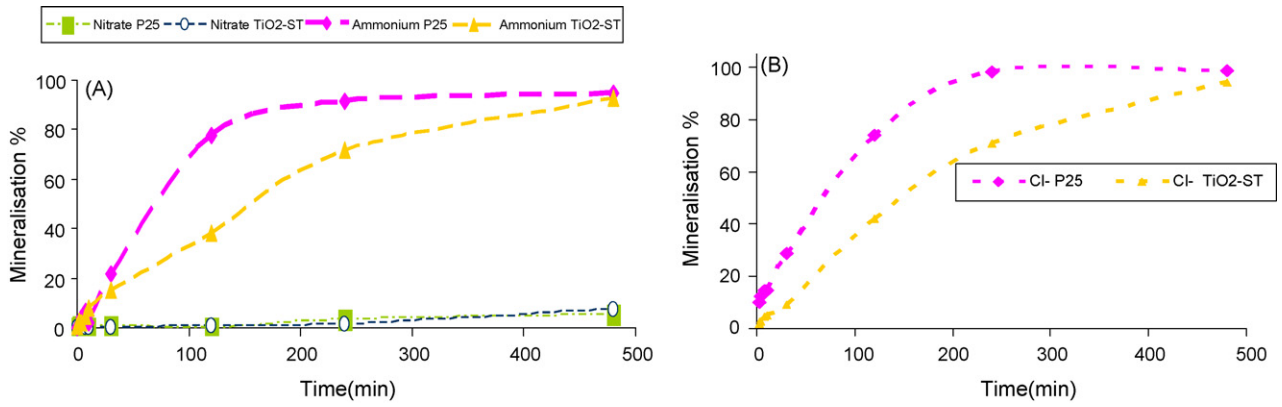

Fig. 3. Evolution of heteroatoms on TiO_2-ST and Degussa P25. (A) Nitrogen evolution (nitrate and ammonium). (B) Chloride ions.

formula, one can expect the formation of NO_2^-, NO_3^- and/or NH_4^+ (regarding nitrogen content in the molecule) as well as Cl^-. The overall equation, valid after long irradiation time in the presence of excess oxygen, which describes photocatalytic mineralization of 3-chloropyridine is presented below:

$$C_6H_4NCl + (15/2)O_2 \rightarrow \text{intermediates} \rightarrow 6CO_2 + NO_3^- + Cl^- + 4H^+$$

Evolution of heteroatoms (nitrate, ammonium and chloride) is depicted in Fig. 3. In agreement with that observed for 3-chloropyridine degradation, mineralization process is faster for P25 though for both systems (TiO_2-ST and P25) mineralization is complete after 8 h irradiation. As regards nitrogen evolution, the main product is ammonium, nitrate only present as minor product 6–12%, in agreement with other studies on photocatalytic degradation of chemicals containing a pyridine ring [8,9]. Finally, nitrite is not observed. Kinetic studies on different initial concentrations of 3-Clpy (not represented) showed that the release rate for chloride is 1.3×10^{-5} mol L^{-1} min^{-1}. The fact that this value is lower than the one found for 3-Clpy disappearance seems to suggest the simultaneous existence of two parallel degradation routes, one involving the initial cleavage of C–Cl bond and another one consisting in the hydroxylation of the aromatic ring prior to the chloride release, though this should be further checked through mass-spectrometry.

As regards CO_2 evolution, TOC measurements confirmed that P25 is more active than TiO_2-ST. Therefore, for instance, 4 h of UV-irradiation resulted in the transformation of 64% of carbon in 3-chloropyridine into CO_2, when TiO_2-ST was used as the catalyst (Fig. 4A) whereas as much as 95% was obtained with Degussa P25 (not represented).

Moreover, CO_2 formation was also followed through on-line connection of the reactor to a GC equipped with a methanator. In this sense, Fig. 4B shows the typical CO_2 profile thus obtained on the example of degradation of 100 ppm of 3-chloropyridine using TiO_2-ST as the photocatalyst. Therefore, CO_2 released reaches a maximum after 50 min of irradiation. The measurement of the area below the curve allows quantification of CO_2. In this case, the area obtained accounts for 97% of expected CO_2. As regards the other 3% CO_2, it was lost through the bubbling of O_2/N_2 mixture through the solution, as confirmed by blank experiments (in the absence of catalyst) monitoring 3-Clpy evolution by HPLC–DAD. Therefore, mineralization was complete for 3-chloropyridine which is important since, otherwise, it could have been transformed into even more pollutant species.

The fact that CO_2 evolution showed a maximum after 50 min of irradiation prompted us to take samples at time intervals below such a value in order to monitor evolution of reaction intermediates by mass spectrometry. In fact, some minor peaks had already been detected in the HPLC–DAD chromatogram at those times, their absorption spectra being quite similar to that of 3-chloropyridine.

3.3. Study of reaction mechanism

In order to identify reaction intermediates different samples were analyzed by GC–MS (direct injection) and SPME–GC–MS. In

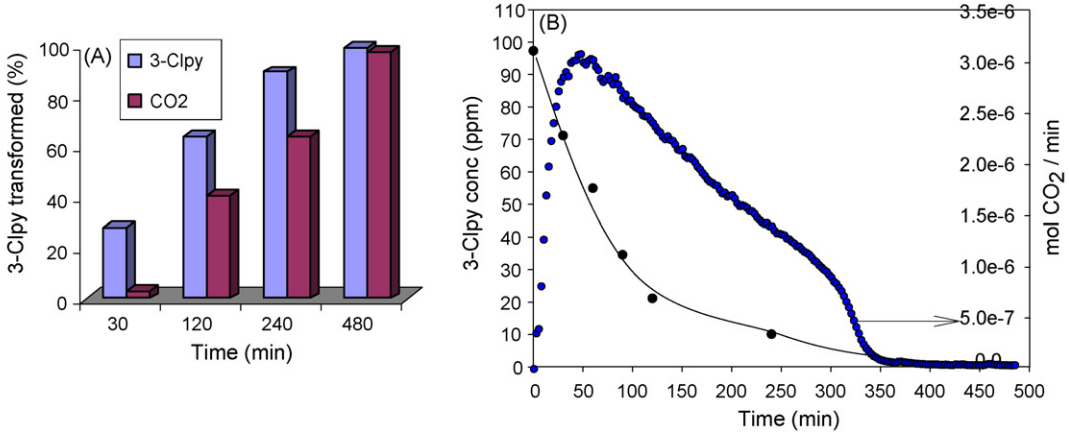

Fig. 4. Photocatalytic degradation of an aqueous solution of 3-chloropyridine (100 ppm) on TiO_2-ST. (A) 3-Chloropyridine disappearance (as monitored by HPLC–DAD) and total organic carbon (TOC) evolution. (B) Monitoring of CO_2 evolution through on-line connection to the photoreactor of a GC with a methanator.

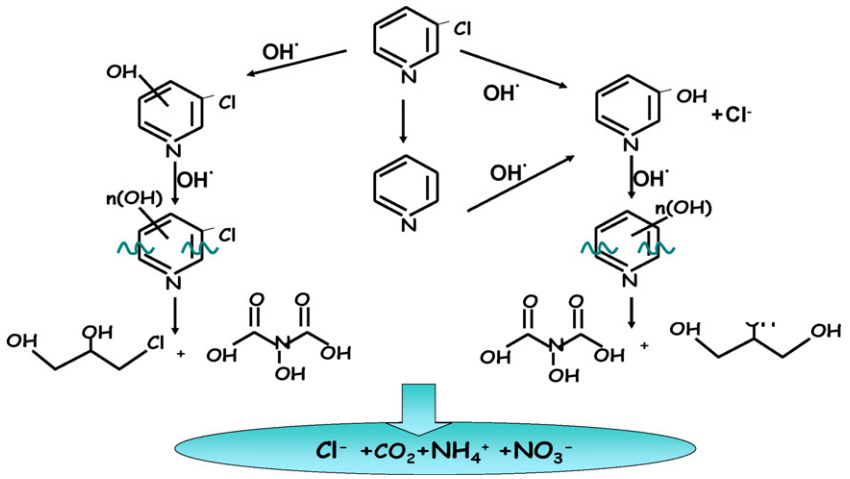

Fig. 5. Tentative degradation pathway proposed for 3-chloropyridine photocatalytic degradation.

view of the results a tentative degradation pathway for 3-chloropyridine disappearance is suggested (Fig. 5). Therefore, the existence of two parallel routes is proposed. Such routes involve hydroxylation and ring opening prior to (left-hand route) or after (right-hand one) the release of chloride ions.

Hydroxylation of the ring prior to the chloride release would explain that 3-chloropyridine disappears at higher rate than chloride species are formed (1.9×10^{-5} mol L^{-1} min^{-1} and 1.3×10^{-5} mol L^{-1} min^{-1}, respectively). Furthermore, un-identified peaks in HPLC–DAD chromatograms of 3-chloropyridine photodegradation, could correspond to hydroxylated chloropyridines, whose absorption spectra will probably be quite similar to that of 3-chloropyridine. Finally, acetic and formic acids were also detected by anionic HPLC.

Having a look at the literature on photocatalytic degradation of pyridine and pyridine derivatives there are discrepancies concerning the reaction mechanism through holes or hydroxyl radicals. Therefore, Agrios and Pichat [10] suggest that pyridine reacts over TiO_2 predominantly via formation of a radical centered on the pyridine ring, its degradation following a pseudo-first-order kinetics. Poulios et al. [11] studied photocatalytic decomposition of herbicide triclopyr proposing the dual hole-radical mechanism, in which direct h^+ oxidation takes place at the oxyacetic group whereas $OH^\bullet$ would attack the pyridine molecule. In our case, detection of pyridine as an intermediate would support mechanism through holes whereas the extraordinary increase in the degradation rate on the bubbling of oxygen through the solution evidences the important role played by hydroxyl radicals.

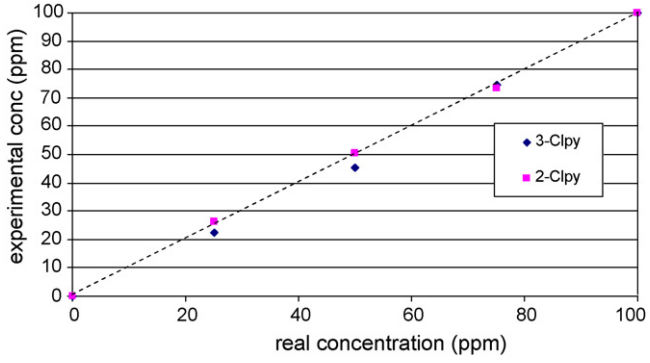

Fig. 6. Results obtained for SPME–GC–MS analyses of different mixtures of 2- and 3-chloropyridine (100 ppm in total) evidencing that both analytes are fully recovered.

3.3.1. Degradation of other chloropyridines: competitive reactions

In a similar way as described for 3-Clpy, 2-Clpy photocatalytic degradation was studied. Interestingly, unlike 3-Clpy, 2-Clpy degradation follows a pseudo-first-order kinetics as shown by Stapleton et al. [12] in a paper published during the preparation of the present manuscript. These results seem to suggest that the existence of a chlorine atom in alpha or beta position with respect to the nitrogen in the pyridine ring results in different reaction mechanisms. One question to answer is whether such different reaction mechanisms would remain the same in competitive reactions, *i.e.* for photocatalytic degradations of aqueous solutions containing both analytes. Monitoring of competitive reactions was performed by SPME–GC–MS. In this sense, the first thing to ensure was that the polyacrylate microextraction fiber did not selectively extract one of the analytes. Therefore, five solutions containing mixtures of 2-chloropyridine and 3-chloropyridine at different concentrations (100 ppm in total) were prepared, extracted with the microfiber and analyzed by GC–MS. Results are shown in Fig. 6. As can be seen, under our experimental conditions, there is complete extraction of both analytes irrespective of their concentration.

The method was then applied to monitor photocatalytic degradation of an aqueous solution containing 50 ppm of both 2-chloropyridine and 3-chloropyridine (Fig. 7). In a first experiment both analytes were added simultaneously and after 20 min

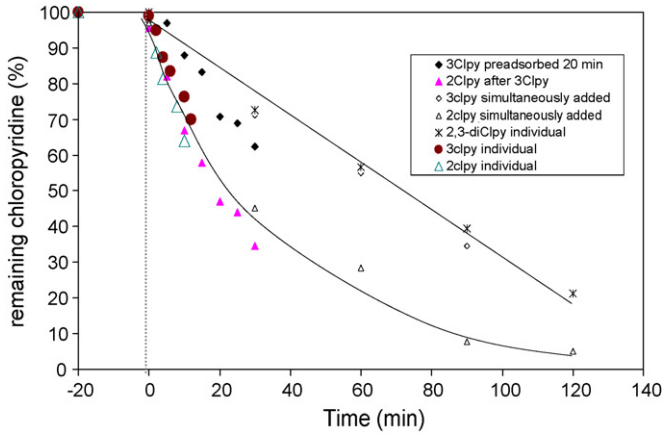

Fig. 7. SPME–GC–MS analyses of individual and competitive reactions of 2- and 3-chloropyridine (50 ppm each) as well as 2,3-dichloropyridine (100 ppm).

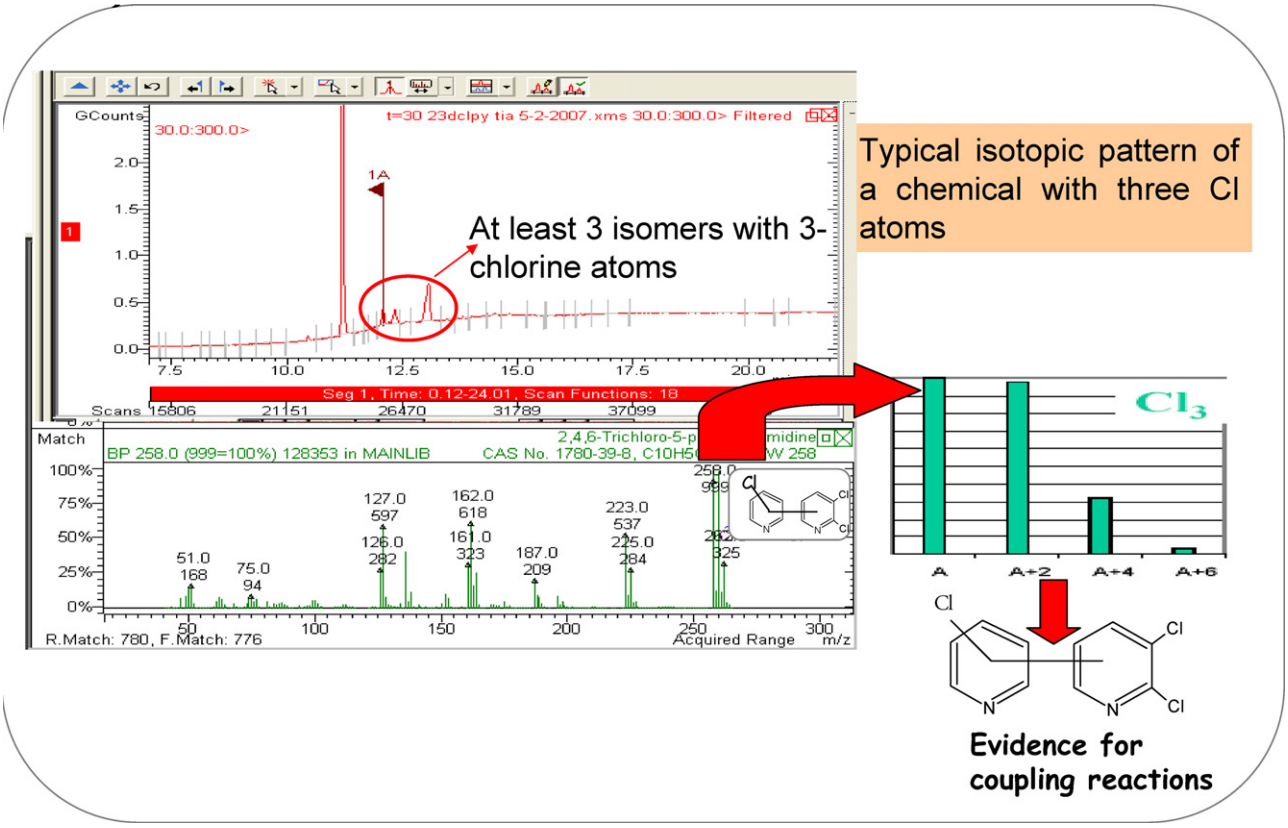

Fig. 8. SPME–GC–MS chromatogram of intermediates obtained in photocatalytic degradation of 2,3-dichloropyridine evidencing a radical mechanism.

of stirring in the dark, light was allowed into the reactor. As can be seen, in a similar way as observed in individual reactions, 2-Clpy and 3-Clpy follow first-order and zero-order kinetics, respectively. A new reaction was then performed where 3-chloropyridine was added first and stirred in the dark with the catalyst for 20 min. Once 3-Clpy had been adsorbed, 2-chloropyridine was added and the lamp was immediately switched on. Under these circumstances adsorption of 3-chloropyridine was favored which resulted in an increase in its photocatalytic degradation. Nevertheless, 2-clpy was still more rapidly degraded. Finally, individual reactions on solutions containing 50 ppm of 3-Clpy or 2-Clpy were performed. In this case, degradation of 3-Clpy proceeded much faster than in competitive reactions whereas that of 2-Clpy was hardly affected. Therefore, it seems that 2-Clpy is strongly adsorbed than 3-Clpy. This constitutes a kinetic orders paradox. 2-Clpy should have a zero-order kinetics reflecting a full coverage of active sites whereas the reverse should be observed for 3-Clpy. It could happen, for instance, that 2-Clpy ring adsorbed vertically on the catalyst surface whereas 3-Clpy did horizontally, thus requiring more catalytic surface and being more sensitive to the co-adsorption of competitors. Nevertheless, this requires further studies (e.g. by ATR spectroscopy).

A final experiment was carried out starting from a solution containing 100 ppm of 2,3-dichloropyridine. In this case, similarly to 3-chloropyridine, degradation follows a zero-order kinetics. Moreover, the detection of coupling products confirmed that it is a radical mechanism. Such products contained 3 chlorine atoms which were easily identified by mass spectrometry due to their typical isotopic pattern (Fig. 8). Detection of coupling reactions in photocatalytic degradation of chloroaromatics has already been reported in the literature [13,14].

The different kinetics observed for 3-Clpy and 2,3-diClpy (zero-order one) or 2-Clpy (first-order one) will probably reflect different reaction mechanisms. Given their basic character, chloropyridines will probably adsorb on TiO_2 as chloropyridinium ions. Chlorine atoms in alpha or beta position with respect to nitrogen in the aromatic ring will change electron density in that ring in a different manner which in turn will result in difference in the reaction mechanism. The different behavior depending on the position of halogens in the aromatic ring has already discussed elsewhere in the case of photocatalytic degradation of chlorophenols [15,16].

4. Conclusions

The above-mentioned results allowed us to draw the following conclusions.

Photocatalytic degradation of 3-chloropyridine was studied on different titania-based catalyst. A first screening allowed us to select two bare-titania systems for further studies. Doping of titania with metals was detrimental for photocatalysis. Under our experimental conditions complete mineralization of 100 ppm of 3-chloropyridine aqueous solution was achieved within 8 h of UV irradiation. Kinetic studies showed a zero-order with respect to 3-chloropyridine. Mechanistic studies carried out by SPME–GC–MS allowed us to propose a degradation pathway consisting of two parallel routes involving hydroxylation of the aromatic ring prior to or after chlorine release. Unlike 3-chloropyridine, 2-chloropyridine degradation follows a pseudo-first-order kinetics. Competitive reactions starting from solutions containing both 3- and 2-chloropyridine evidenced the stronger adsorption of the latter which resulted in a partial inhibition of the degradation of 3-chloropyridine in its presence. Finally, degradation of 2,3-chloropyridine follows a zero-order kinetics. The use of SPME–GC–MS to monitor reaction intermediates allowed us to detect coupling products thus evidencing a radical mechanism.

Acknowledgments

The authors wish to acknowledge financial support from the Consejería de Educación y Ciencia of the Junta de Andalucía (Projects FQM 191 and P07-FQM-2695) and the Spanish Ministerio de Educación y Ciencia (Projects CTQ 2005-04080/BQU and CTQ2007-65754, co-financed with FEDER funds). Finally, Dr. Colmenares is thankful to the Spanish Ministerio de Educación, Cultura y Deportes for a post-doctoral fellowship and A. Marinas to Junta de Andalucía for a contract.

References

[1] A. Aranzábal, J.A. González-Marcos, R. López-Fonseca, M.A. Gutierrez-Ortiz, J.R. González-Velasco, Stud. Surf. Sci. Catal. 130B (2000) 1229.
[2] M.A. Aramendia, V. Borau, I.M. García, C. Jiménez, A. Marinas, J.M. Marinas, F.J. Urbano, C. R. Acad. Sci. II 3 (2000) 465.
[3] P. Bhatt, M. Kumar, M. Suresh, S. Mundliar, T. Chakrabarti, Crit. Rev. Environ. Sci. Technol. 37 (2007) 165.
[4] L. Zhang, S. Sawell, C. Moralejo, W.A. Anderson, Appl. Catal. B 71 (2007) 135.
[5] J.-M. Herrmann, Catal. Today 53 (1999) 115.
[6] J.C. Colmenares, M.A. Aramendía, A. Marinas, J.M. Marinas, F.J. Urbano, Appl. Catal. A 306 (2006) 120.
[7] S. Bakardjieva, J. Šubrt, V. Štengl, M.J. Dianez, M.J. Sayagues, Appl. Catal. B 58 (2005) 193.
[8] B.F. Abramović, V.B. Anderluh, A.S. Topalov, F.F. Gaál, Appl. Catal. B 48 (2004) 213.
[9] M.A. Aramendia, A. Marinas, J.M. Marinas, J.M. Moreno, F.J. Urbano, Catal. Today 101 (2005) 187.
[10] A.G. Agrios, P. Pichat, J. Photochem. Photobiol. A 180 (2006) 130.
[11] I. Poulios, M. Kotsitzi, A. Kouras, J. Photochem. Photobiol. A 115 (1998) 175.
[12] D.R. Stapleton, D. Mantzavinos, M. Papadaki, J. Hazard. Mater. 146 (2007) 640.
[13] J.-C. D'Oliveira, C. Minero, E. Pelizzetti, P. Pichat, J. Photochem. Photobiol. A 72 (1993) 261.
[14] C. Minero, E. Pelizzetti, P. Pichat, M. Sega, M. Vincenti, Environ. Sci. Technol. 29 (1995) 2226.
[15] D. Robert, S. Parra, C. Pulgarin, A. Krzton, J.V. Weber, Appl. Surf. Sci. 167 (2000) 51.
[16] S.P. Parra, Doctoral Thesis, École Polytechnique Fédérale de Lausanne, 2001.